

MIRIAH - ROSÆ Math Model Annex A

Microwave **I**nterferometry **R**adiating **I**ncrementally **A**ccumulating **H**olography
(MIRIAH)

Non Proprietary Version for Internet

A parametric analysis of MIRIAH's signal performance.

By William H. Grisham, President
ROSÆ Inc.
Columbine Village, Unit #205
7901 W. 52nd Ave.
Arvada, CO 80002
February 7, 2007

This 17 page document is prepared on,
and calculated in Mathcad 7 format, and
is the Proprietary Intellectual Property of
ROSÆ Inc. who retain all Patent rights.
Only those individuals named in the
Disclosure Agreement with ROSÆ Inc.
are authorized to read this document.

Non Proprietary Version for Internet

INTRODUCTION

This Math Model addresses only the architectural level of the MIRIAH technology. It is designed to give a feasibility level of proof only. This is realistic, since systems level engineering will require hundreds (if not thousands) of engineering hours, at a cost which is beyond the reasonable expected potential resources of the inventor, Bill Grisham. MIRIAH grows in increments from a two satellite version (MIRIAH*2), to MIRIAH*3 or MIRIAH*4, to MIRIAH*6, to MIRIAH - ROSÆ (consisting of 12 Satellites, comprising MIRIAH technology plus Communication and Navigation technology). Whereas, this present work addresses only MIRIAH's RF Imaging. The reader is cautioned to evaluate this work on that basis only. This present document will disclose the basic Interferometrically illuminated microwave signal parametric analysis for a single coherent recording in detail, and then extrapolate this heuristically to the fully multiplexed set to be encountered only when MIRIAH*6 to MIRIAH - ROSÆ arrives on the scene. The reader must understand the 3-D holographic recording will not be enabled until MIRIAH - ROSÆ is operational (some time after MIRIAH*3 - which enables only conventional 2-D imaging at first).

Therefore, this present parametric analysis starts off with the assumption we are at the level of MIRIAH*3, in which there are three interconnected VLBI (Very Long Baseline Interferometers), forming a VLA (Very Large Array), as a triad of VLBI distributed as an equilateral triangle in space. The VLA's 2-D plane is isometric (fixed inertially perpendicular to an axis, which bisects ROSÆ's three orthogonal orbital plane intersections). This plane (and its VLA), is one of eight such planes in the full ROSÆ architecture. This present analysis assumes the architecture uses the 5:1 resonant orbits, which are optimum for MIRIAH - ROSÆ. Therefore, since coherence is maintained continuously, the 5:1 resonant record repeats itself, so there will be a multiple overlay of holographic sets, each of which forms a sector of the accumulating phase record, or Matched Filter (MF). As this process continues **it remains in analog form** (it is digitized **after** the real image is formed) even though in appearance it is a hologram comprised of millions of "zone plates", each centered on millions of pixels. These "zone plates" of an isentropic radiating object (like a sphere) will look like Figure 4, but many objects will have huge fluctuations in reflectance and corresponding variations in their MF. This rich 3-D and "glint" detail is one of the great benefits of holography - increasing the identification detection certainty.

Each of these holograms (the "perfect" spatially referenced MF) is capable of reconstruction into a rotateable 2-D image. But, when multiplexed into the full ROSÆ architecture, this will distribute 16 of these VLA holographic records into ROSÆ's 8 isometric planes, which circumscribe the globe (capable of 3-D imaging). Since these planes are all at an equal angle, the multiplexed set will be conformal. Then, if a pixel is not "fully filled" near the apex of any one of VLA, it will pick up the rest of its "fill" from an adjacent VLA. But, in the present analysis, for clarity, we will assume the case of a pixel located near a VLA center, since at the center a pixel is "fully filled" within that one MF. So each "fully filled" hologram (a 2-D MF) is the basis for a 2-D real Aperture. This is a complete departure from SAR's 1-D Synthetic Aperture, with far reaching implications, e.g., a 2nd Power-Aperture (2nd PA) is also enabled downstream of the 1st PA's output at the Fourier Plane (the MF). Then we must compute SNR at the output of the 2nd P.A. (in the image plane - **not the MF**). Further, coherence is only present upstream of the A/D point (the Analog to Digital transformation **stops phase aggregation**), and is why all SAR must compute SNR at the receiving antenna, and can use only one PA (within the SAR's imaging system). This is one of several "break through" differences in performance between MIRIAH and SAR. For MIRIAH does not have a synthetic aperture, rather it has **many real apertures** (i.e., each MF is a hugely diverse lens set focusing a real image). Hence, SAR experts should accept the conclusions reached on Page 16, which shows why SAR analytic techniques are irrelevant in this technology.

The radius of the earth (meters): $Re := 6.38 \cdot 10^6$

The angular velocity of the earth (rad/sec): $\omega_e := 7.292 \cdot 10^{-5}$

The gravitational acceleration (m/sec²): $g_e := 9.7993$

Preferred orbit angular velocity (rad/sec): $\omega_o := 5 \cdot \omega_e$

The central radius of the orbit (from the earth's center in meters): $\rho_o := \sqrt[3]{\frac{Re^2 \cdot g_e}{\omega_o^2}}$

The orbit's altitude: $h_o := \rho_o - Re$

The wavelength, λ , is iterated manually. (The reader is invited to exercise the math model by changing λ).

$\lambda := .25$ meters

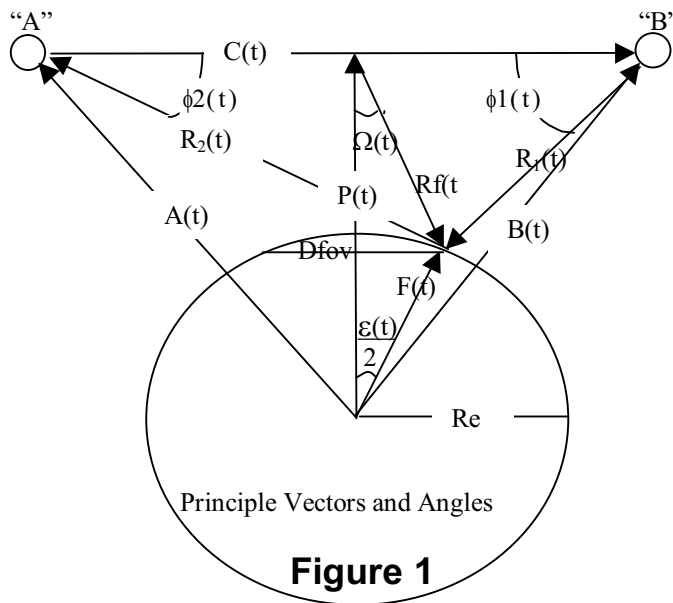
For hologram sector "fill"

time (or "dwell time", TD),

from t_1 to t_2 , we (arbitrarily) set:

$$t_{mid} := \frac{\pi}{4 \cdot \omega_o} \quad t_1 := 0.75 \cdot t_{mid} \quad t_2 := 1.25 \cdot t_{mid}$$

$$TD := t_2 - t_1 \quad TD = 1.077 \cdot 10^3 \quad \text{seconds}$$



Set vector range to: $i := 1..3$

$$\text{Satellite "A" vector: } A(t) := \rho_o \cdot \begin{bmatrix} \cos(\omega_o \cdot t) \\ 0 \\ \sin(\omega_o \cdot t) \end{bmatrix} \quad \text{Satellite "B" vector: } B(t) := \rho_o \cdot \begin{bmatrix} 0 \\ \sin(\omega_o \cdot t) \\ \cos(\omega_o \cdot t) \end{bmatrix}$$

The VLBI vector: $C(t) := B(t) - A(t)$

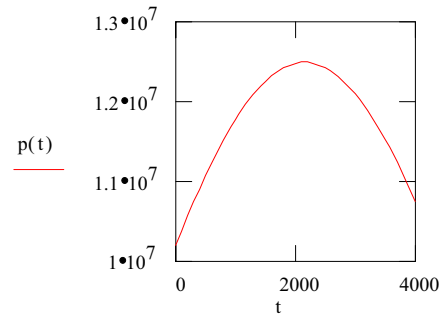
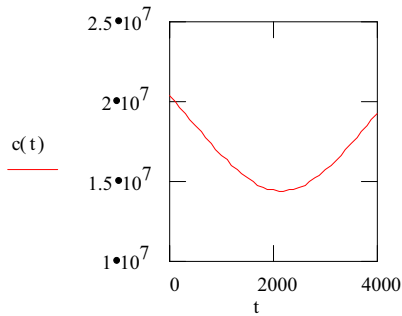
$$\text{The magnitude, "c(t)", of vector "C(t)", is: } c(t) := |C(t)| = \rho_o \sqrt{2 - \sin(2\omega_o t)}$$

VLBI's Phase
Centerline vector
"P(t)", is:

$$P(t) := \left(\frac{A(t) + B(t)}{2} \right) \text{ has magnitude } p(t) := |P(t)| = \frac{\rho_0 \sqrt{2 + \sin(2\omega_0 t)}}{2}$$

For a range of time values for t we set: $t := 0, 100 \dots 4000$ since $2 \cdot t_{\text{mid}} = 4.308 \cdot 10^3$

NOTE: A 4,000 second time interval covers about 90° of orbit ("t" is 308 seconds "short" of 90°) so we get a representative graph spread here, yet, without excessive grid lines:



The angular momentum, M_C (a vector), of the VLBI: $M_C = C(t) \times \dot{C}(t)$

$$M_C := \rho_0^2 \cdot \omega_0 \cdot \begin{bmatrix} -1 \\ -1 \\ -1 \end{bmatrix} \text{ of magnitude: } |M_C| = \rho_0^2 \omega_0 \sqrt{3} \text{ fixed in space, along this isometric axis: } \begin{bmatrix} -1 \\ -1 \\ -1 \end{bmatrix}$$

The angular velocity (vector) is fixed along the same isometric axis: $\omega_C(t) := \frac{M_C}{c(t)^2}$ or $\omega_C(t) := \frac{\omega_0}{(2 - \sin(2 \cdot \omega_0 \cdot t))} \cdot \begin{bmatrix} -1 \\ -1 \\ -1 \end{bmatrix}$

And similarly for vector $\omega_P(t)$: $\omega_P(t) := \frac{\omega_0}{(2 + \sin(2 \cdot \omega_0 \cdot t))} \cdot \begin{bmatrix} -1 \\ -1 \\ 1 \end{bmatrix}$ (on an adjacent isometric axis)

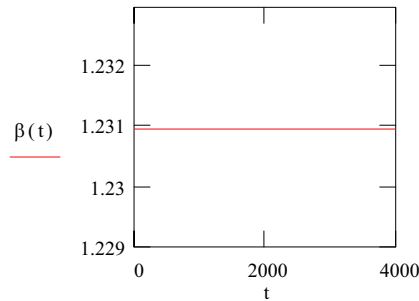
The magnitudes of $\omega_C(t)$ and $\omega_P(t)$ are respectively: $w_C(t) := \frac{\omega_0 \cdot \sqrt{3}}{(2 - \sin(2 \cdot \omega_0 \cdot t))}$ $w_P(t) := \frac{\omega_0 \cdot \sqrt{3}}{(2 + \sin(2 \cdot \omega_0 \cdot t))}$

See ε in Fig. 1 (solving first for components ε_C and ε_P): $\varepsilon_C := \int_{t_1}^{t_2} w_C(t) dt$ $\varepsilon_P := \int_{t_1}^{t_2} w_P(t) dt$

Let β be the angle between the planes normal to $\omega_C(t)$ and $\omega_P(t)$:

$$\beta(t) := \arccos \left(\frac{\omega_C(t) \cdot \omega_P(t)}{|\omega_C(t)| \cdot |\omega_P(t)|} \right) \quad \beta(0) = 1.230959 \quad \text{radians}$$

in which $\beta(t)$ is constant, as the angular momentum is constant.



$$\beta_{\text{deg}}(t) := \beta(t) \cdot \frac{180}{\pi} \quad \beta_{\text{deg}}(0) = 70.529 \quad \text{degrees}$$

Then by Law of Cosines in Spherical Trig:

$$\varepsilon := \text{acos} \left[\left(\cos(\varepsilon_c) \cdot \cos(\varepsilon_p) \right) + \left(\sin(\varepsilon_c) \cdot \sin(\varepsilon_p) \right) \cdot \cos(\beta(0)) \right]$$

$$\varepsilon = 0.62 \quad \text{radians} = \quad \varepsilon \cdot \frac{180}{\pi} = 35.529 \quad \text{degrees}$$

$$D_{\text{fov}} := 2 \cdot R_e \cdot \sin\left(\frac{\varepsilon}{2}\right) \quad \text{is the diameter of the FOV in meters}$$

The vector "F(t)" in Figure 1 is:
$$F(t) := \text{Re} \cdot \left[\left(\frac{P(t)}{|P(t)|} \cdot \cos\left(\frac{\varepsilon}{2}\right) \right) + \left(\frac{C(t)}{|C(t)|} \cdot \sin\left(\frac{\varepsilon}{2}\right) \right) \right]$$

The two (bistatic) range vectors:
$$R1(t) := F(t) - B(t) \quad \text{and} \quad R2(t) := A(t) - F(t)$$

The two (bistatic) range magnitudes:
$$Rn1(t) := |R1(t)| \quad \text{and} \quad Rn2(t) := |R2(t)|$$

$R_o(t)$ is the vector from the center of the FOV to "A"
$$R_o(t) := A(t) - \frac{\text{Re} \cdot P(t)}{|P(t)|}$$

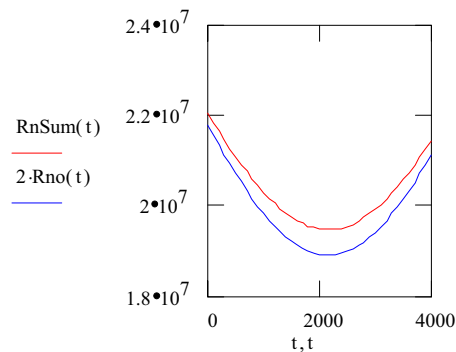
$R_{no}(t)$ is the magnitude of range from either Satellite to the center of the Field of View (FOV):
$$R_{no}(t) := |R_o(t)|$$

The total bistatic range, $RnSum$ is:
$$RnSum(t) := Rn1(t) + Rn2(t)$$

From this graph, it is evident the signal arriving at the receiving antenna has its leading edge from the FOV center, and its trailing edge from the FOV edge.

The "look" or sample time, $Till(t)$, rasters radially from center to edge (in about 2 milli-secs when t is at midpoint in its "pass"):

$$Till(t) := \frac{RnSum(t) - 2 \cdot Rno(t)}{3 \cdot 10^8} \quad \text{seconds}$$



Pages 6 to 14 are not included in this abridged version of the Signal Margin Math Model for Proprietary Protection of more sensitive pages.

This Math Model uses normal inverse square law propagation methods, with conservative assumptions for: Losses (L), Radar Cross Sections (RCS), Band Width (B), Noise Temperature (T), normalized reflectivity (σ), and a far field antenna structure for a very wide beam width subtending the earth's limb so side lobes do not reflect from the FOV (they point outward to space).

Of course there are some similarities and differences between SAR's image digital reconstruction of 2-D images, and MIRIAH's analog aggregation of its Matched Filter (MF) and subsequent reconstruction of its 3-D holographic imagery via illumination of the MF by much higher laser frequencies (than the illumination frequency). SAR uses *Chirp/Compression* and *Integrates Power Density* into an Energy Density increase (a Gain). Whereas, MIRIAH aggregates the MF over much longer coherence time (an analog *integration*) and then adds energy density by illuminating the MF with much shorter wavelengths and much smaller mapped area (an energy density *compression* or Gain).

After the first 24 hours of operation, MIRIAH's VLBI centerlines trace out a coverage grid, each cell of which is a very small fraction of the total illumination coverage area of the "fully filled" MF. So we can assume the energy density is uniform at the MF when "fully filled". So the energy density Gain is simply the compression in area, which makes Gain simple to calculate. This is analogous to SAR Chirp/Compression, but MIRIAH has two coherent streams (an *area* compression). As energy is conserved, and we have calculated Energy Density, and each pixel's zone plate covers the entire MF, then the Gain of the MF is the disc/pixel area ratio. Or, equivalently it is the FOV area divided by the resolved ground area (see page 17).

The Model also calculates Doppler, Pass Band, Disc Raster Rates, Clutter, MF fill rate, % of overfill, estimates SNR for very large bright objects upstream of the MF, SNR per stage, etc.

.

Interferometer fringe width considerations, per Bragg's Law.

Each VLBI's bistatic angle, $\phi_3(t)$, at the FOV is: $\phi_3(t) := \pi - \phi_1(t) - \phi_2(t)$

Per Bragg's Law, the VLBI's fringe interval, $d_{\text{fringe}}(t)$, (at ground level) of the FOV is: $d_{\text{Fringe}}(t) := \frac{\lambda}{\phi_3(t)}$

Calculating this as a function of wavelength: $d_{\text{FringePer}\lambda}(t) := \frac{1}{\phi_3(t)}$

Ground resolution of each VLBI, $\text{VLBI}_{\text{Res}}(t)$, is: $\text{VLBI}_{\text{Res}}(t) := \frac{h(t) \cdot \lambda}{c(t)}$

Calculating this as a function of wavelength: $\text{VLBI}_{\text{ResPer}\lambda}(t) := \frac{h(t)}{c(t)}$

Resolution at the **center** (at $t_{\text{mid}} = 2,150$ secs) is determined by fringe interval at the **edge** (at $t = 0$), as follows:

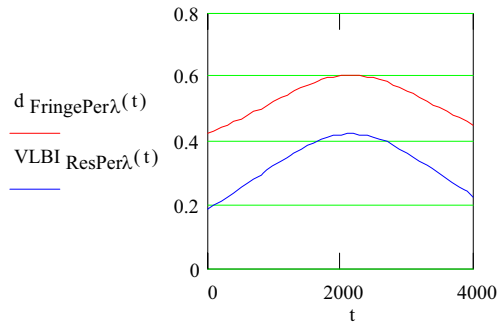
$$d_{\text{FringePer}\lambda}(0) = 0.4$$

Fringe interval at the **edge** of the Fourier Plane

lines up with:

$$\text{VLBI}_{\text{ResPer}\lambda}(t_{\text{mid}}) = 0.4$$

VLBI resolution at the **center** of the Image Plane



"This shows that the resolution is the same as the fringe interval, and so the matched filter (MF) is a collage of millions of "Zone Plates" (like Fresnel lenses in the Fourier Plane), each of which is centered over a pixel in the image plane (see Figure 4 below, which is extracted from Fig. 7c of the "Introduction to Scientists" Document). And, as the above graph shows, each of these "Fresnel lenses" covers an area equal to the entire FOV (scaled down to the disc's size). In those cases where the pixels are near the boundary between of the mapping plates, the "Zone Plate" will continue on into the next (conformal) plate.

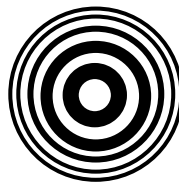


Figure 4

A Fresnel lens or "Zone Plate" is formed on the disc and centered over each pixel as the Matched Filter "fills". (See also the graph and explanatory text at the bottom of page 8 of the Math Model "A Parametric Analysis of MIRIAH's swath coverage).

Comparing fringe interval vs. resolution, shows resolution depends significantly on the bistatic angle, $\phi_3(t)$, and so on the magnitude of $[VLBI / D_{FOV}]$. Then we conclude **all short baseline Interferometers and SAR will be aliased (indeterminate) for large FOV**. Hence, it is clear why MIRIAH is **uniquely viable** for this Mission Requirement, as it is "unaligned" and has a positive 2nd P.A. Gain**, while illuminating a very large FOV, as required to meet a large "Supply" for a **profitable** Commercial Service. Then we conclude **only MIRIAH satisfies these interrelated economical and technological limitations on this Mission Requirement.**

(*NOTE: see "Positive Gain", Figure 6, "Introduction to MIRIAH for Scientists").

For, as the FOV increases, the "Zone Plate" or "Fresnel" lens **area** in Figure 4 increases, while the fringe interval at its outside edge decreases and so the **resolution gets finer**. And since area increases, **then the Gain increases**. Or (again), since resolution of the matched filter (MF) is dependent on the parametric relation shown in Figure 3 above, as $c(t)$ or the size of the VLA increases, the resolution will get finer, while the Gain will increase. Then at midpoint, when $t = 2158$ seconds, $c(t)$ is at its minimum, and so Gain is at a minimum (as can be verified in the above graphs on the MF Gain). This is why MIRIAH will be such an economic success. For, as the FOV increases, "Supply" increases, but the illuminating energy density at the FOV decreases, yet the increasing Gain tends to compensate, keeping "Costs" low.. And, since resolution improves, then "Demand" increases. Hence, MIRIAH is a huge benefit/cost improvement over SAR, since its high "Demand" & "Supply" match up with low "Cost".

This ends the parametric analysis of MIRIAH's 1st PA (at microwave frequencies). The 2nd P.A. is at optical (probably laser) frequencies. Although **SNR, P_{Trans} , and ground resolution will not change**, the optical gain will **not** be the same as the microwave coherent gain, G_{holo} . Also, since the Noise Density is dominated by the earth's 290 degree Kelvin temperature, the optical system will add only negligible noise density. And, since the 2nd P.A.'s optical "burn in" time, $T_{Optical}$, and average illumination power, $P_{Optical}$, is at the discretion of the designer (not constrained by T_{ill}), then the $SNR_{Optical}$ will be equal to the $SNR_4(t)$ when the following optical design's energy level is imparted to (work done on) a typical disc area, A_D (in meters²):

$$P_{Optical} \cdot T_{Optical} \geq 60 \cdot \frac{\int_1^2 E3(t) dt}{TD} \cdot \left(\frac{F_{Optical}}{F_{Microwave}} \right)^2 \cdot A_D \quad \text{watt-seconds}$$

$E3(t)$ is the energy density per VLBI during one "pass", of duration, TD. But there are 2 data streams arriving at Satellite "C" from both "A" and "B", and there are 10 revisits per day, and 3 VLBI per VLA, or a total of 60 times $E3(t)$ when the VLA is "fully filled". Therefore, we conclude MIRIAH is completely, and easily feasible, at very low energy and cost levels, and so its Mission Requirement is also completely feasible - both technically and economically. During the systems R&D, we will also investigate losses due to disc "read" entropy, which may lower SNR one order of magnitude (work out during "read" = work in during "write", less entropy).

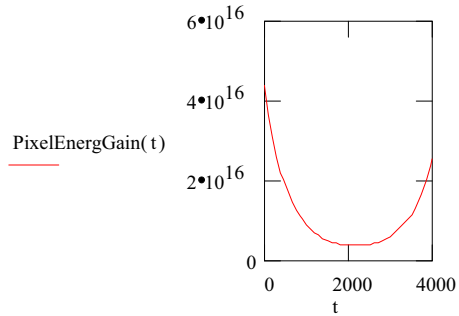
Considerations on matching startup "Demand" to "off the shelf" components

We recognize the optical 2nd P.A. is the more powerful stage and is easily feasible in view of MIRIAH's evolution from SARA, which is "perfectly" linear, orthogonal, conformal, stable, pre-focused over a large depth of field for a rotating spherical object FOV to a disc, etc. (See *NOTE below). However, at first we may opt to use digital processing when the SNR is positive at the Fourier Plane for large planar objects (see Pages 14 - 15). For the market "Demand" will be low at first, and while an all digital 2nd P.A. will have far lower capacity than an optical 2nd P.A., it may be preferred at startup, as its lower capacity may be enough for lower initial "Demands".

*NOTE: All previous optical processors for SAR used asymmetrical optical components (e.g., conical lens segments, etc.), as all SAR use a "flat earth" model. Whereas, MIRIAH's evolution from SARA will enable conventional optical components (e.g., conventional convex and concave lenses, etc.). So MIRIAH's optical R&D will be simple yet precise (whereas early SAR used optical methods which were very complicated), and immediately downstream of the optical "read" **we will of course go digital** (with all of the advantages of modern computers).

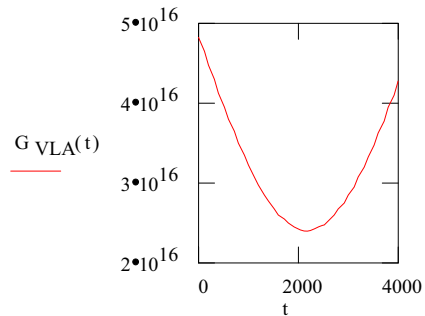
The "Bragg's Law" discussion on pages 14 to 15 (see Signal Performance Dec 28 06.mcd), shows the pixel is illuminated in the Fourier Plane as a Fresnel lens (as in Fig 4) **across the entire MF format**. Since the energy density Gain in the transformation from the Fourier to Image plane replicates the accumulated illumination energy of the FOV area to the point resolved in the FOV (during T_{coh}), then the number of ground resolved pixel areas in the FOV must be the same as the Gain of the MF. So this simply says the MF's gain is the same as the VLA's Gain would be **if** it were a 2-D Synthetic Aperture. Comparing $G_{MF}(t)$ with PixelEnergyGain(t) in this graph, one sees they equate. So each pixel's MF is as Bragg's Law proves, i.e., a "Zone Plate" or Fresnel Lens, as in Fig. 4. And we note this Gain would be very close to the Gain computed for a "fully filled" VLA as shown next with this standard antenna Gain method for $G_{VLA}(t)$:

$$\text{PixelEnergyGain}(t) := \frac{(\text{FOV}_{\text{seen}}(t))}{D_{\text{res}}(t)^2}$$



This shows our MF equates to a "fully filled" VLA as if it were for a 2-D SAR. So, by replacing the Synthetic Aperture and moving its **equivalent Gain** to small discs (or other random access high density memory), **invites nano technology**, with its manifold improvements. For, SIR-C antenna's 12m aperture = 51 wavelengths (illuminated at 0.23 m/λ) to the MF's 130,000 wavelengths (Laser illuminated at 0.7 μm/λ). This proves MIRIAH's MF apertures, when comparing normalized apertures (in wavelengths), are also far greater than SIR-C's ("Smaller is Bigger" in modern IT technology).

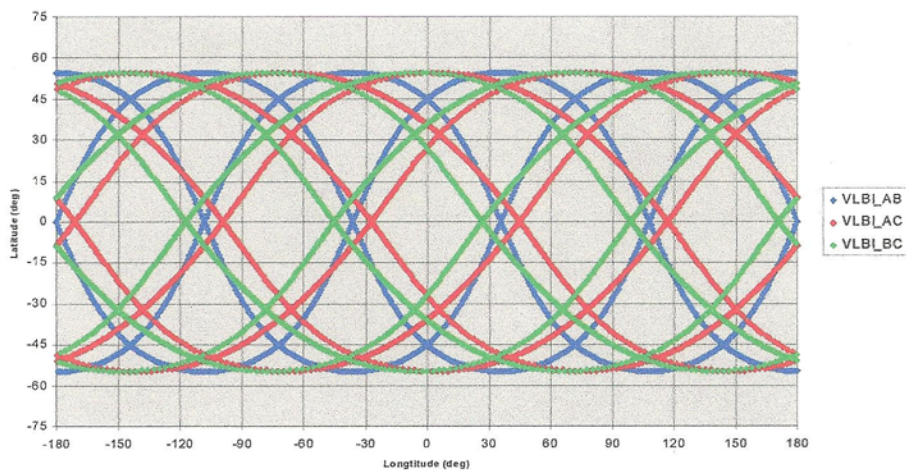
$$G_{VLA}(t) := \frac{4 \cdot \pi \cdot A_{VLA}(t) \cdot \eta}{\lambda^2}$$



Considerations Relating To MIRIAH's Tactical "Near Real Time" Interferometer Coverage Rate vs. SAR's Extremely Slow Coverage Rate.

Below are FOV centerline traces per Sidereal Day for MIRIAH*3, using only 1 swath. Multiple swaths are the rule (from 4 to 8 since ROSAE - MIRIAH's symmetry leads to common universal joint couplings - all with constant Angular momentums, which in the 12 satellite case cancel about the yaw and roll axes, while adding to the pitch axis for ideal stability for "belly down" attitude for earth viewing. Even with only one swath MIRIAH*3 has this coverage density:

VLBI Center Traces



Note there appear to be gaps in the coverage for MIRIAH*3. But this coverage diagram displays only the centerline traces, not the **huge** illuminated areas for **Interferometers**, which cover the entire visible surface (**whole Continents**). Hence, for MIRIAH*3, these thinner coverage areas will be completely "filled" in at the hologram - a Matched Filter (or MF), due to the illumination beam width's **huge** coverage area. And, thinner areas in this figure will be **8 times denser** for MIRIAH*6 and **32 times denser** for ROSAE - MIRIAH. Also, their hologram "fill time" will be **much faster** (11 min. for MIRIAH*6, and 3 min. for ROSAE - MIRIAH's 12 Satellites). While, for a SAR with its small 1-D coherent Gain (only ≈ 35 dB), power requirements are prohibitive, and "Full filled" delay is in **days and weeks**. Furthermore, MIRIAH's 2-D and 3-D Coherent Gain (≈ 160 dB) is about a **Billions of times larger** than SAR's. So MIRIAH is inexpensive, timely, completely practical, easily feasible, and MIRIAH enables timely **Tactical** missions, while SAR can only serve untimely Strategic missions (noting that true information is highly perishable).

NOTE: These coverage rates will be cut in half for manmade objects, like cars and buildings, which are symmetrical about one axis. For objects which are symmetrical about two axes, like missiles, the time will be cut in half again.

So the price paid by SAR and its single Power-Aperture is too high for another reason, for with two P.A., the first P.A. **can maintain phase closure** so that the second P.A. **can use much longer coherence times (thousands of times longer)**. Typically, SAR experts (who are used to 3 second coherence) challenge MIRIAH's feasibility for this reason, and in this way hold up progress. For by hugely increasing coherent Gain, MIRIAH can then greatly reduce the physical Gain without sacrificing a very high overall Gain, and thereby take advantage of larger beam widths, to get faster "fill times", to get a Tactical mission enabled for our country and the world. For we believe in mission first consistent with both lower costs, and practicality. This is why and how we have succeeded.